Dynamic correlation functions in quantum many-body systems at zero temperature

E. R. Gagliano and C. A. Balseiro
Centro Atómico Bariloche, Instituto Balseiro, Comisión Nacional de Energía Atómica, 8400 San Carlos de Bariloche, Rio Negro, Argentina
(Received 21 June 1988)

We present a simple numerical approach to compute dynamic correlation functions in quantum many-body systems at zero temperature. The method is based on a projective technique for the memory-function formalism, and requires as a starting point an independent evaluation of the ground-state energy and wave function. We illustrate the method with a one-dimensional model of spinless fermions and calculate the density-density, current-current, and single-particle correlation functions. The obtained spectral functions show different types of elementary excitations: particle-hole, soliton-antisoliton, exciton, etc. We compare our results with analytical results, and with those obtained through different approaches available in the literature.

I. INTRODUCTION

In the last few years many numerical methods have been developed to study the thermodynamic and ground-state properties of quantum many-body systems.[1] However little progress has been made in the development of numerical methods to deal with the real-time or real-frequency dynamics of such systems.[2] A first attempt was made by Hirsch and Schrieffer who proposed a method to compute real-frequency correlation functions using a Monte Carlo–like algorithm.[3] They dealt only with one degree of freedom systems and have given reasonable results only after an exceedingly large number of Monte Carlo steps. Alternative methods have been developed to evaluate real-time correlation functions directly and to make analytic continuation of the imaginary-time results for these simple systems.[4] Considering the enormous amount of computation time required, it seems difficult to apply these methods to quantum many-body systems.

Schütler and Scalapino propose a least-squares fitting procedure to evaluate real-frequency correlation functions of many-particle systems.[5] This approach is basically a procedure to extract real-frequency self-correlation functions from the corresponding imaginary-time Green's functions of many-particle systems that can be simulated by standard quantum Monte Carlo techniques. The use of this technique to evaluate correlation functions quantitatively would again imply prohibitive amounts of computational time.

Recently, we have presented a simple method to compute dynamical correlation functions in quantum many-body systems at zero temperature.[6] The approach is based on a projective technique for the memory-functions formalism.[7] We have previously given a brief description of the method.[6] Here we present a detailed discussion of the technique along with results for a variety of different types of correlation functions.

The organization of the paper is as follows: In Sec. II we describe some general properties of dynamic correlation functions along with the proposed approach. In Sec. III we illustrate the algorithm using as a test a simple spinless fermion model. We calculate the density-density, current-current, and single-particle dynamical correlation functions. Final comments are included in Sec. IV.

II. DYNAMICAL CORRELATION FUNCTIONS AND METHOD

The linear response $A(t)$ of a many-body system at zero temperature to an externally applied field $\varepsilon(t')$ can be written in terms of the correlation function

$$C_{AB}(t-t')=\langle \psi_0 | A(t)B(t') | \psi_0 \rangle , \tag{1}$$

where $B(t')$ is conjugated to $\varepsilon(t')$, $A(t)$ is the Heisenberg representation of A, and $|\psi_0\rangle$ is the ground state of the system. Many experiments, like inelastic neutron scattering and nuclear magnetic resonance, measure directly the Fourier transform $C_{AB}(\omega)$ of $C_{AB}(t-t')$, the imaginary part of which is given by

$$C''_{AB}(\omega)=\sum_n \langle \psi_0 | A | \psi_n \rangle \langle \psi_n | B | \psi_0 \rangle \delta(\omega+E_0-E_n) . \tag{2}$$

The summation is taken over all the eigenstates $|\psi_n\rangle$ of the Hamiltonian H with energy E_n. E_0 is the ground-state energy. A characteristic feature of $C''_{AB}(\omega)$ is that it has a peak at a frequency equal to the energy of some excitations of the system. Of particular interest is the case of self-correlation functions, $B=A^\dagger$, for which $C''_{AA}(\omega)$ is a real and positive function. If the operator A is also Hermitian, $C''_{AA}(\omega)$ is an even function. Then, we only need to calculate, for example, the spectra for positive frequencies. The real part of $C_{AB}(\omega)$ can be obtained from the imaginary part using the Kramers-Kroning relations.

From the computational point of view, the spectral representation Eq. (2) is not faithful, because it needs a complete knowledge of the eigenvectors and eigenvalues of H. Different analytical algorithms have been developed to deal with the calculation of dynamical

correlation functions. However they are based on perturbative series or on a chain of coupled equations which are difficult to solve. Although many approximated schemes have been proposed, $C_{AB}(\omega)$ is frequently calculated with uncertain approximations. Numerical methods become a powerful tool for the study of dynamical properties, from which we can evaluate effective interactions and single-particle self-energy, and then use these to proceed with analytic calculation of the properties of the particle-hole and particle-particle responses.

To obtain the dynamical correlation function, we define

$$G_A(Z)=\langle\psi_0|\,A^\dagger(Z-H)^{-1}A\,|\psi_0\rangle\ ; \tag{3}$$

clearly $G_A(Z)$ is a matrix element of the resolvent operator $(Z-H)^{-1}$. The relation between $C_{AA}(\omega)$ and $G_A(Z)$ is easily obtained as

$$C_{AA}(\omega)=-\frac{1}{\pi}\mathrm{Im}[G_A(\omega+E_0+i\eta)]\ , \tag{4}$$

where η is a small positive number. As in the Haydock, Heine, and Kelly approach to obtain local density of states in tight-binding models, the resolvent $G_A(Z)$ can be written as a continued fraction,[8]

$$G_A(Z)=\cfrac{\langle\psi_0|\,A^\dagger A\,|\psi_0\rangle}{Z-a_0-\cfrac{b_1^2}{Z-a_1-\cfrac{b_2^2}{Z-\cdots}}}\ . \tag{5}$$

The coefficients a_n and b_n can be evaluated from the moments $\mu_n=\langle\psi_0|\,A^\dagger H^n A\,|\psi_0\rangle$.[9] A recurrence relation between these moments and the coefficients was used by the authors of Ref. (10) to study the dynamical properties of spin $-\frac{1}{2}$ XY and transverse-Ising models at infinite temperature. For more complicated many-body systems this approach is not useful numerically, because the moments increase rapidly with n. Therefore, the recurrence relation between $\{a_n,b_n\}$ and μ_n becomes very sensitive to numerical error, and for large systems high-precision calculations (33 significant figures) are not enough. We found it convenient to evaluate the coefficients by a projective technique for the memory-function formalism.[7,11] The advantage of this method is that it avoids the use of recursion relations. The method can be summarized as follows: (1) define the state $|\psi_0\rangle=A\,|\psi_0\rangle$; (2) generate a set of orthogonal states with the relation

$$|f_{n+1}\rangle=H\,|f_n\rangle-a_n\,|f_n\rangle-b_n^2\,|f_{n-1}\rangle\ ;$$

and (3) evaluate the coefficients a_n and b_n:

$$a_n=\langle f_n\,|\,H\,|\,f_n\rangle/\langle f_n\,|\,f_n\rangle\ ,$$

$$b_{n+1}^2=\langle f_{n+1}\,|\,f_{n+1}\rangle/\langle f_n\,|\,f_n\rangle,\quad b_0=0\ .$$

With this procedure we can evaluate a large number of coefficients $\{a_n,b_n\}$ and construct the continued-fraction expression for $G_A(Z)$. Obviously for implementing the procedure described above we need as a starting point the ground-state energy and wave function. Because we are studying finite-size systems, the resolvent $G_A(Z)$ has a discrete spectrum, the main feature of which is that it has a finite number of poles at some excitation energy of the system. Note that in the pictures we broaden the δ peaks by the inclusion of a finite η.

III. ILLUSTRATIVE EXAMPLE

To test the method, we have calculated the density-density, current-current, and single-particle correlation function for a one-dimensional model of spinless fermions. The Hamiltonian is given by

$$H=-t\sum_{i=1}^{N}(c_i^\dagger C_{i+1}+C_{i+1}^\dagger C_i)+G\sum_{i=1}^{N}n_i n_{i+1}+\Delta\sum_{i=1}^{N}(-1)^i n_i\ , \tag{6}$$

where $C_i^\dagger$ creates an electron at site i and $n_i=C_i^\dagger C_i$ is the number operator. We consider a half-filled band and use different types of boundary conditions. The Hamiltonian H can be mapped, using the Wigner-Jordan transformation,[12] into an anisotropic spin-$\frac{1}{2}$ Heisenberg model with a staggered magnetic field Δ. This model was used in Ref. (13) to describe some properties of one-dimensional charge transfer compounds and in Ref. 14 to study the electronic structure of high-T_c superconductors. For $\Delta=0$, the system shows an instability at $G=2t$. If $G<2t$ the charge is uniformly distributed in the ring, the system is conducting, and for $N\to\infty$, the excitation spectrum is a gapless continuum. For $G>2t$ the ground state is a charge ordered state in which the expectation value of the charge at two neighboring sites alternates between $\frac{1}{2}(1+\delta n)$ and $\frac{1}{2}(1-\delta n)$. For $N\to\infty$, the ground state is doubly degenerate and is separated by a gap from a continuum.[15]

For $G=0$ and $\Delta\neq0$, the Hamiltonian Eq. (6) can be easily solved in the momentum space using the usual canonical transformation to new quasiparticle creation operators for the conduction and valence bands.[16] In terms of the quasiparticle operators the Hamiltonian H reads

$$H=\sum_k E_k(A_k^\dagger A_k-B_k^\dagger B_k),\quad E_k=(\Delta^2+4t^2\cos^2k)^{1/2}\ , \tag{7}$$

where A_k (B_k) destroy an electron in the valence (conduction) band with momentum $k=2\pi l/N$, $l=0,\pm1,\pm2,\ldots,N/4$. Clearly, the conduction- and valence-quasiparticle energies are E_k and $-E_k$, respectively. In the ground state the valence states are filled and the conduction states are empty; then, the system is an insulator with a gap equal to $2(\Delta^2+4t^2\cos^2k_F)^{1/2}$. For $N\to\infty$, $k_F\to\pi/2$ and the gap is 2Δ. The value of the gap can be increased by the Coulomb interaction G. For nonzero G and Δ the Hamiltonian H cannot be diagonalized exactly in the $N\to\infty$ limit. However, different numerical approaches can be used to obtain information about the ground-state properties of finite systems. In this work, we diagonalize rings with different values of N. The exact diagonalization of H is performed by using a recently

developed modified Lanczos method.[17] This procedure which we will use to generate the ground-state wave function has been described in detail in Ref. 17.

In what follows we calculate different correlation function corresponding to Hamiltonian Eq. (6) in order to show the power and accuracy of the method described in Sec. II.

A. Density-density correlation function

The density-density correlation function is defined as

$$C_n(k,t)=\langle n_k(t)n_k\rangle \tag{8}$$

with

$$n_k=\frac{1}{\sqrt{N}}\sum_l e^{-ikl}(n_l-\tfrac{1}{2}) .$$

From the Wigner-Jordan transformation we identify Eq. (8) as the S_z-S_z dynamical spin correlation function for the isomorphic spin problem. This function is directly related to the inelastic neutron scattering cross section.[18] The Fourier transform of $C_n(k,t)$ has an interesting representation. For $G=0$ and $\Delta=0$, the spectral decomposition is easily obtained and the imaginary part is given by

$$C_n^{\parallel}(k,\omega)=\frac{\pi}{N}\sum_p (1-f_{p+k})f_\eta\delta(\varepsilon_{p+k}-\varepsilon_p-\omega) , \tag{9}$$

where f_p is the zero temperature Fermi function and $\varepsilon_p=-2t\cos p$ with $p=2\pi n/N$, $n=0,\pm1,\ldots,N/2$. For small momentum transfer, $k\ll\pi$ the spectrum is narrow and its center is approximately at $\omega\sim 2kt$. As k increases, more and more lines appear distributed over an energy range up to the band with $4t$. The number of peaks at a given k is determined by the number of particle-hole excitations, whose momentum differ in k from the ground-state momentum. The maximum number of peaks is obtained for $k=\pi$.

We have evaluated the correlation function $C_n^{\parallel}(k,\omega)$ for different values of G and $\Delta=0$. We study rings of different sizes up to $N=20$. For different sizes we use periodic or antiperiodic boundary conditions. The numerical errors depend on the value of k and on the number of sites N. However, the largest error is smaller than 2%.

In Fig. 1 we present the results for a system of 16 sites in the noninteractive limit. The exact result, Eq. (9), is not included in the figure because in the scale used it could not be distinguished from the numerical results. For comparison we also display the Monte Carlo histograms of Ref. 5. The results clearly show the correct behavior. For small k, a single peak at low frequency appears corresponding to an electron-hole excitation across the "Fermi surface." As k is increased we found more structure in the spectra which completes at $k=\pi$. The line at $\omega=0$ obtained for $k=\pi$ corresponds to the promotion of a particle from $-k_F$ to k_F ($k_F=\pi/2$). Clearly, the Monte Carlo results are qualitatively correct. However, they cannot reproduce the spectrum when it has a more fine structure. This is a consequence of the approximation introduced in the Monte Carlo procedure, the least-square fitting of the two lowest moments of the spectra.

In the strong-coupling regime, the infinite system has a twofold-degenerate ground state. The two states differ only in the phase of the charge-density wave (CDW). For $t=0$, the Hamiltonian is diagonal in the site representation. The lowest excited states for $\Delta=0$ have soliton-antisoliton pairs. Each pair increases the energy by an amount equal to G. Therefore, the spectra consist in peaks at nG with $n=0,1,2,\ldots$ So for $t\ll G$ and $\Delta=0$, the spectrum consist of bands centered at $G,2G,3G,\ldots$. A detailed lowest-order calculation of $C_n(k,\omega)$ for $t\ll G$ and $\Delta=0$ has been carried out in Ref. 19. For $N\to\infty$, the density-density correlation function is given by

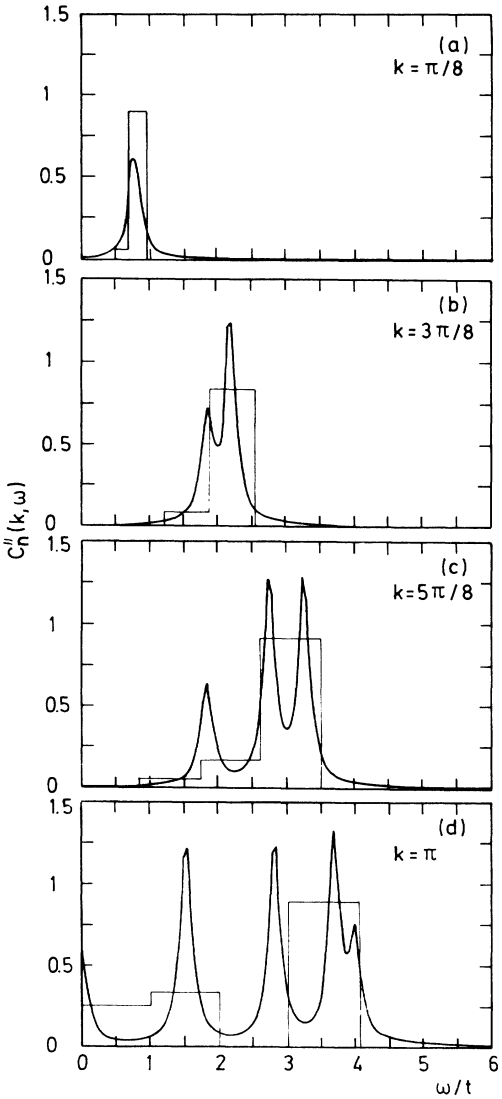

FIG. 1. Real-frequency-density correlation function of a noninteracting half-filled 16-site chain. ($G=0$, $\Delta=0$, $\eta=0.1t$) with periodic boundary condition. Thin line, Monte Carlo results; heavy line, present approach.

$$C_n^{\parallel}(k,\omega)\approx\begin{cases}\dfrac{8t^2}{G^2}\dfrac{\sin^2(k/2)}{\Gamma(k)/2}\left[1-\left[\dfrac{\omega-G}{\Gamma(k)/2}\right]^2\right]^{1/2} & \text{for } \omega^-\le\omega^+\le\omega\ ,\\ 0 \quad \text{otherwise}\ , \end{cases} \tag{10}$$

where $\Gamma(k)=\mid 8t\cos 2k\mid$ and $\omega^{\pm}=G\pm\Gamma(k)/2$. In Fig. 2 we plot the obtained results for $G=6t$ on a half-filled 16-site chain with periodic boundary conditions. All the structure shown in this figure corresponds to a single soliton-antisoliton pair. For comparison we also display in the figure the Monte Carlo results.[5] It should be noted that the Monte Carlo simulations give good qualitative results in the strong coupling regime. As is shown in Fig. 2, for a given k, we obtain a band centered at G with a width approximately of $\Gamma(k)$. For $k=\pi$, we also found a peak at $\omega=0$ since the operator n_k with $k=\pi$ connects the two degenerate ground states. All these results are in qualitative agreement with strong-coupling calculation. In addition, we expect to see similar absorption peaks around $\omega\sim 2G,3G,\ldots$ but their intensities are very small. To show the power of the algorithm used here we plot in Fig. 3, the real-frequency density correlation function in a large ω scale. A second band centered around $\omega\sim 2G$ shows up very clearly corresponding to excitations with two soliton-antisoliton pairs. The intensity of this second band is two orders of magnitude smaller than the first one, therefore a simulation using Monte Carlo techniques requires high statistics and in consequence enormous amounts of computational time. In Figs. 4 and 5, we display our calculations, on a half-filled ring of 16 and 20 sites using periodic and antiperiodic boundary conditions, respectively. Also we show the strong-coupling result Eq. (10). As we can see from Fig. 4, the strong-coupling result qualitatively describes the spectra; however, for $k\neq\pi$, small peaks appear out of the strong coupling band. Therefore, the lowest-order strong-coupling result is, at best, qualitatively correct. For a quantitative description, the interband mixing would have to be taken into account. In Fig. 5, we plot the density correlation function for $k=\pi$ and $G=4t$, $6t$, and $8t$. It can be noticed that the strong-coupling predictions represent qualitatively well the numerical exact result.

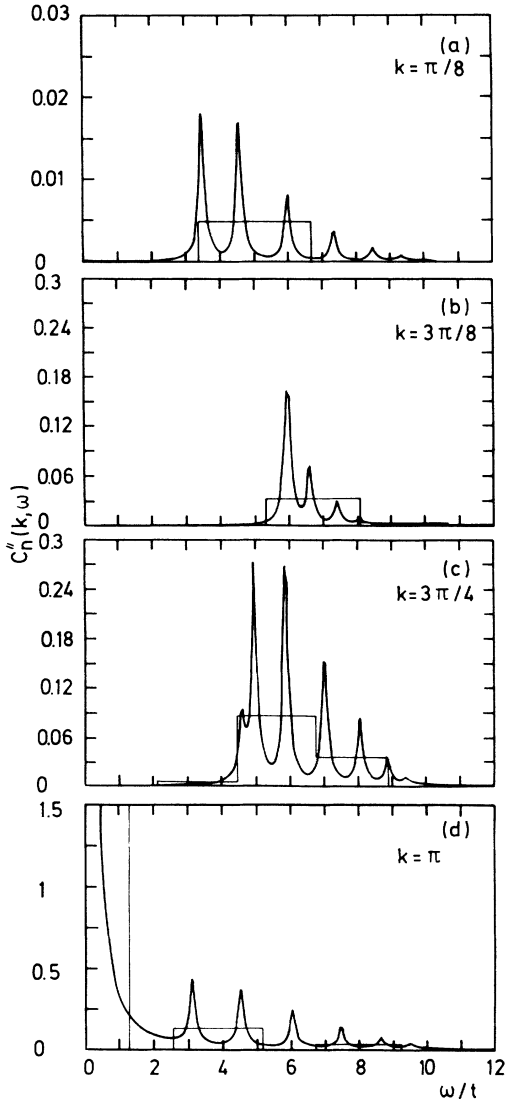

FIG. 2. Real-frequency-density correlation function of a strongly interacting half-filled sixteen-site chain; $G=6t$, $\Delta=0$, $\eta=0.1t$, with periodic boundary conditions. Thin line, Monte Carlo results; heavy line, present approach.

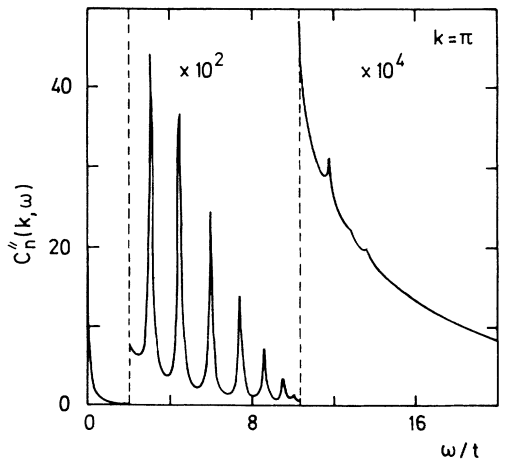

FIG. 3. Real-frequency-density correlation function of a strongly interacting half-filled 16-site chain with periodic boundary condition; $G=6t$, $\Delta=0$, $\eta=0.1t$.

Another interesting question about the density correlation function follows: Which are its features when we remove one fermion from the CDW ground state of the half-filled system?. The new system has a soliton-antisoliton pair in its ground state, therefore the excitation spectrum differs significantly from the half-filled case. Due the inelastic scattering from a single soliton as well as the scattering from the soliton pair, the real-frequency density function has more structure at low frequencies than in the half-filled case.[20] In Fig. 6 we show the results for $G=6t$ on a 16-site ring with 7 fermions and periodic boundary conditions. It indeed differs drastically from the half-filled case. We also show the Monte Carlo results which again describe qualitatively the overall feature of the spectrum.

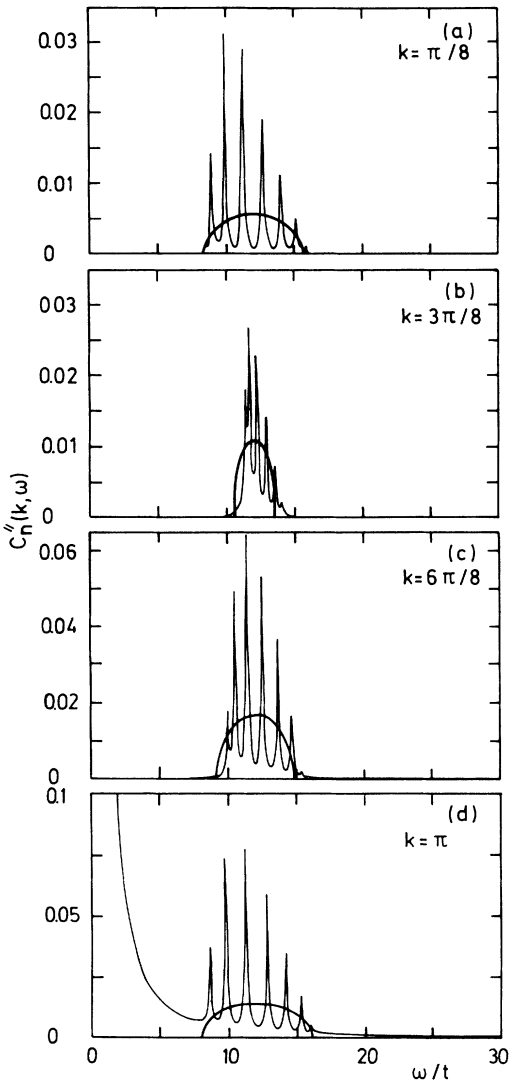

FIG. 4. Comparison of the real-frequency-density correlation function obtained with the present approach and a strong coupling calculation. Half-filled 16-site ring with periodic boundary condition; $G=12t$, $\Delta=0$, $\eta=0.1t$.

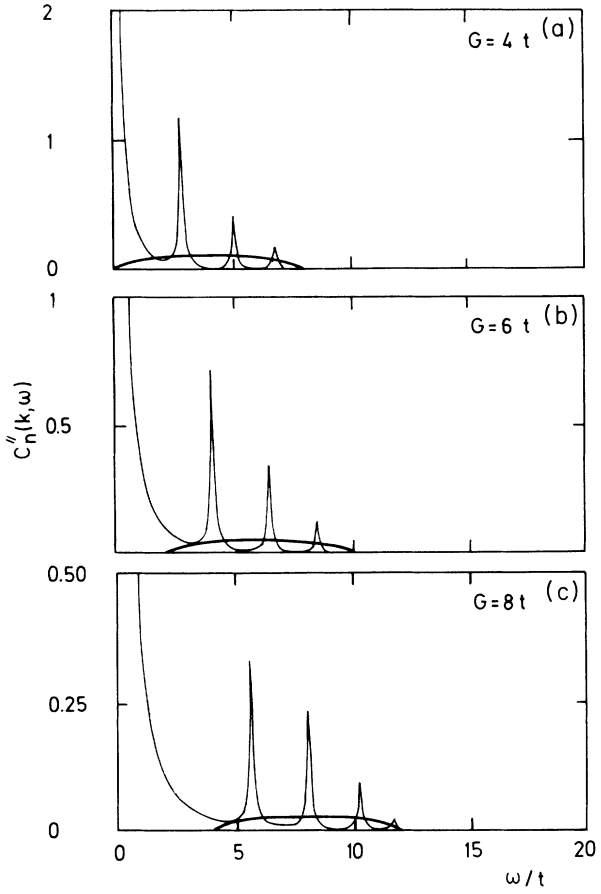

FIG. 5. Real-frequency-density correlation function at $k=\pi$ for different values of G. Half-filled 20-site ring with antiperiodic boundary condition; $\Delta=0$, $\eta=0.1t$.

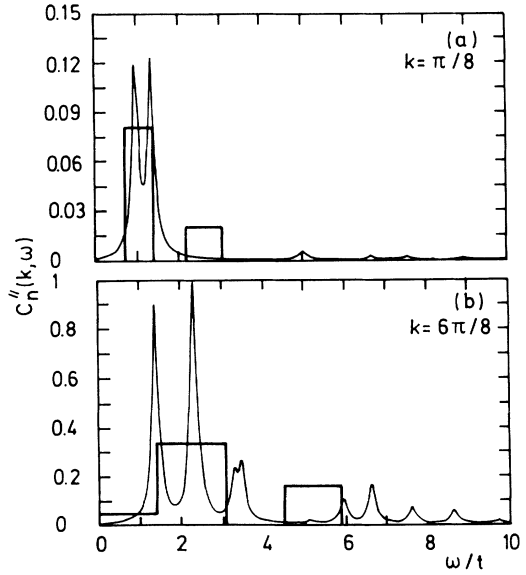

FIG. 6. $C_n^{\parallel}(k,\omega)$ for a strongly coupled less-than-half-filled system; $G=6t$, $\Delta=0$, and $\eta=0.1t$. Thin line, Monte Carlo results; heavy line, present approach.

B. Single-particle correlation function

The single-particle correlation function is defined as

$$G_j(t) = -i\Theta(t)\langle\{C_j(t), C_j^\dagger\}\rangle \ , \tag{11}$$

where $C_j^\dagger$ create an electron at site j and $\Theta(t)$ is the Heaviside function. The imaginary part of the Fourier transform of $G_j(t)$ is related with the spectra measured in x-ray photoemission spectroscopy (XPS) and bremsstrahlung isochromat spectroscopy (BIS) experiments.[21] For $G=0$, the imaginary part of $G_j(t)$ can be easily obtained as

$$\begin{aligned}\mathcal{D}_j(\omega) &= \frac{-1}{\pi}\mathrm{Im}G_j(\omega) \\ &= \frac{1}{N}\sum_k \left[\left[1-(-1)^j\frac{\Delta}{E_k}\right]\delta(\omega+E_k)\right. \\ &\quad \left. + \left[1+(-1)^j\frac{\Delta}{E_k}\right]\delta(\omega-E_k)\right] \ ; \end{aligned} \tag{12}$$

clearly the spectral function $\mathcal{D}_j(\omega)$ has a gap of order 2Δ, separating the conduction and valence band. From Eq. (12) we see that the odd sites have more weight in the valence band than do the even sites. For $\Delta=0$ and $G\neq 0$, $G>2t$, the spectral function $\mathcal{D}_j(\omega)$ is qualitatively similar to the $\Delta\neq 0, G=0$ case; however the origin of the gap is very different. From $\mathcal{D}_j(\omega)$ we can calculate the energy gap. Clearly a finite-size system always has a gap, its determination is very useful in studying the gap at $N\to\infty$ or in finding other excitations. This point is the subject of the following section.

In Fig. 7, we show results for $G=0, \Delta=t/4$ in a half-filled 12-site chain with antiperiodic boundary conditions. The gap obtained from $\mathcal{D}_j(\omega)$ coincides within five significant figures with the exact one, $2(\Delta^2+4\cos^2 k_F)^{1/2}$, $k_F=5\pi/12$. This result was used as a test of our program. In Fig. 8, we show the results obtained for a half-filled 16-site chain with antiperiodic boundary condition. $\mathcal{D}_j(\omega)$ has a rich structure and shows a gap. The peaks

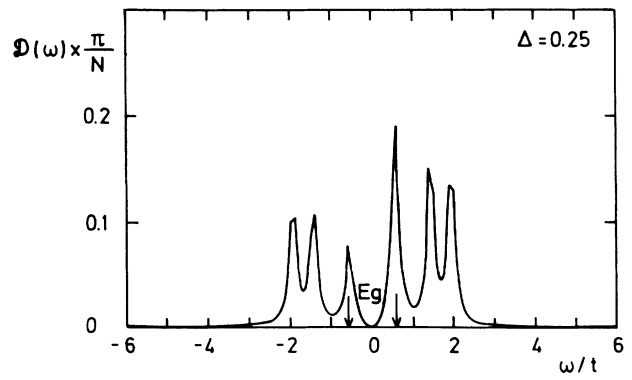

FIG. 7. Spectral function $\mathcal{D}_j(\omega)$ at even site j for a half-filled chain of 12 sites with antiperiodic boundary conditions. $G=0$, $\Delta=1/4t$, $\eta=0.1t$.

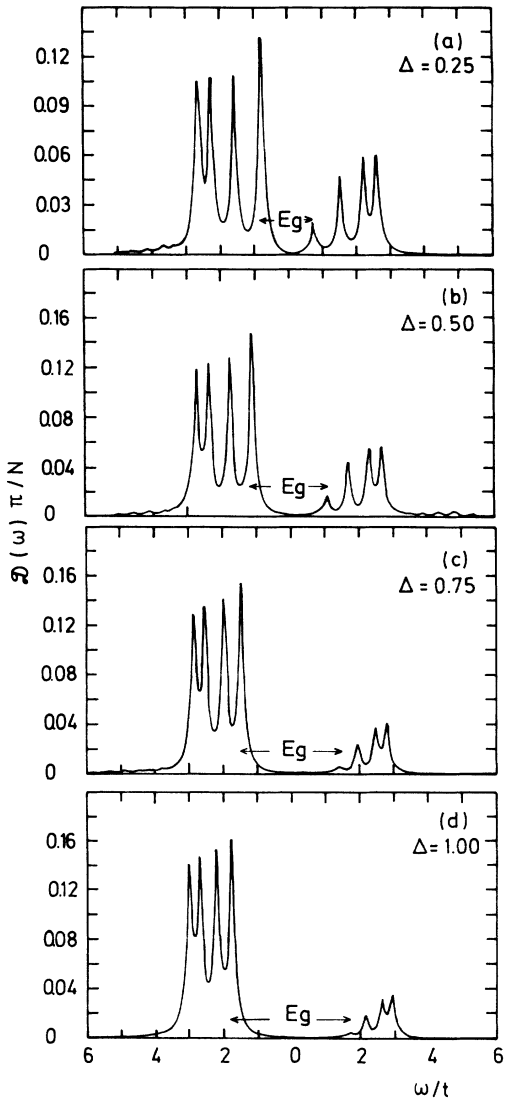

FIG. 8. Spectral function $\mathcal{D}_j(\omega)$ at even site for a ring of 16 sites for different values of Δ; $G=t$, $\eta=0.1t$.

correspond to electron or hole excitations with frequency equal to $E_0(N/2)-E_n(N/2\pm 1)$, where $E_0(N/2)$ is the ground-state energy of the system with $N/2$ particles and the $E_n(N/2\pm 1)$ are the energies of the states when the system has $N/2\pm 1$ particles. For $\Delta=0$, a broad gap is found for $G>2t$. This result is in agreement with the exact solution of the model. For $\Delta\neq 0$, the structural gap 2Δ is increased by the Coulomb interaction G as is shown in Fig. 8. Summarizing, a careful calculation of $\mathcal{D}_j(\omega)$ allow us to obtain the gap for a given parameter set.

C. Current-current correlation function

We define the current-current correlation function as

$$\mathcal{J}(t) = \langle J(t)J(0)\rangle \ , \tag{13}$$

where

$$J(0) = -i\sum_l (C_l^\dagger C_{l+1} - C_{l+1}^\dagger C_l) \tag{14}$$

and $J(t)$ is the current operator in the Heisenberg representation. This function allows us to obtain information about the excitation spectrum of the system with a fixed number of particles. The lowest-lying optical excitation is a charge transfer of an electron from an even site to a neighboring site. For $t=0$, the excitation energy is $(2\Delta+G)$. In the same limit, the particle-hole gap,

$$E_0(N/2+1)+E_0(N/2-1)-2E_0(N/2)=E_g$$

is $2\Delta+2G$. Therefore, the energy of the charge-transfer excitation is lower than the particle-hole gap by an amount equal to G. This charge-transfer excitation corresponds to a tightly bound particle-hole pair or Frenkel exciton. Because this pair is an excitation of the half-filled system, the only way to see it is by the measure of the absorption spectrum which is the most powerful method of obtaining information about the charge-transfer excitations. This spectrum cannot be calculated directly and easily by quantum Monte Carlo techniques. The method presented in this paper allow us to obtain directly the Fourier transform of $\mathcal{J}(t)$, $\mathcal{J}(\omega)$. In Figure 9 we plot the imaginary part of $\mathcal{J}(\omega)$ for different values of Δ obtained for a half-filled 16-site chain with antiperiodic boundary conditions. The spectral function $\mathcal{J}(\omega)$ has a pole when ω is the energy of the exciton E_0. It also has poles corresponding to other excited states with energies higher than the electron-hole excitation. From Fig. 9 we find that E_0 is lower than the electron-hole gap, E_g as obtained from Fig. 8. The binding energy of the exciton is $E_b=E_g-E_0$. For $\Delta \gg t$ the binding energy is approximately given by[13]

$$E_B \sim 4G\,|\rho-\tfrac{1}{2}|-G\ , \tag{15}$$

where ρ equals the number of holes in the even sites.[22] This limit corresponds to the case where the electron-hole pair is almost completely localized in two sites of the chain. Therefore, the exciton has a small radio. For $\Delta \ll t$ and $G<2t$, the binding energy is[13]

$$E_B \sim 4G^2(\,|\Delta|+2G\,|\rho-\tfrac{1}{2}|\,)/p^2t^2\ , \tag{16}$$

where $p=1+G/t\pi$. In this limit the exciton radius is much larger than the lattice parameter.

In Fig. 10, we plot the binding energy E_B as a function of Δ for $G=t$. We also display the extended and localized limits. The dots in the figure were obtained using finite size scaling techniques for the sequence $N=6,8,10,12,14,16$ in half-filled systems using periodic (antiperiodic) boundary condition for $N/2$ odd (even). Using a least-squares fitting procedure, $E_B \sim A+B/N+C/N^2$, we obtain the binding energy E_B^{∞} for the $N\to\infty$ limit. Clearly the numerical results are a smooth interpolation between the weak and the strong coupling regime.

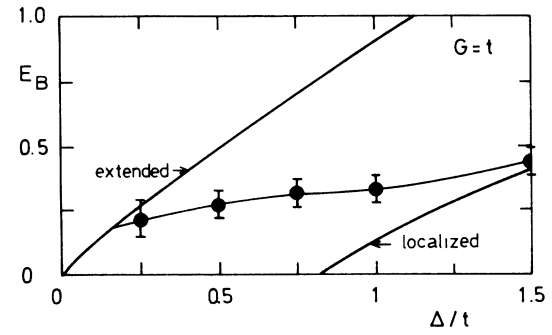

FIG. 10. Extrapolated exciton binding energy as a function of Δ/t for $G=t$. We also include the strong and weak coupling limits, Eqs. (15) and (16).

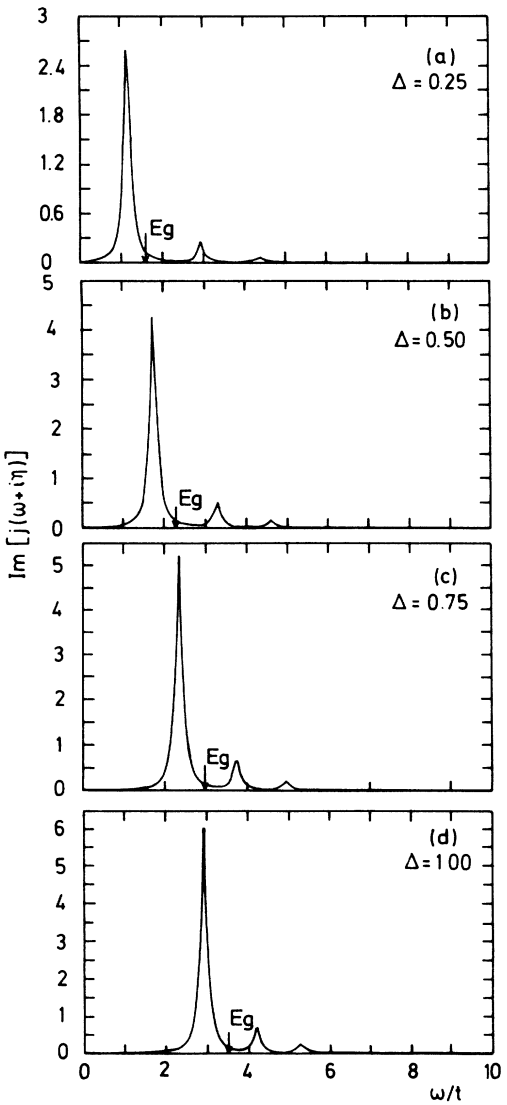

FIG. 9. Real-frequency current-current correlation function for different values of Δ; $N=16$, $G=t$, and $\eta=0.1t$.

IV. CONCLUSION

In this paper we have analyzed different dynamical correlation functions using a Lanczos-like algorithm. The only requirement for its implementation is an accu-

rate calculation of the ground-state energy and wave function. To test and illustrate the method, we have applied it to a simple one-dimensional model of spinless fermions.

We have calculated the density-density, current-current and single-particle dynamical correlation functions. The obtained spectral functions show different types of elementary excitations—particle-hole, solitonic, and excitonic—and allow us to gain information about some static properties such as the energy gap and the binding energy of the exciton. The results show that the method has enough accuracy as to apply finite size scaling to calculate static properties.

We believe that we have demonstrated the utility of the presented approach in numerical calculations at zero temperature. It will be a challenging problem to extend the algorithm to nonzero temperature.

Directly carrying over our techniques to nonzero temperature appears to be quite costly in terms of computer time. The algorithm is appropriated for the study of the dynamics of spin systems and fermions in a lattice. With our computing facilities, (a VAX 11/780), the dynamical properties of spin-$\frac{1}{2}$ Heisenberg systems with $N \leq 24$ and of the extended Hubbard model with $N \leq 12$ can be evaluated in moderate computing time. For large systems, larger and faster computing facilities would be required. However, a pruning of the Hilbert space can be used as an approximate approach for large systems. This approximation provides accurate results only at low frequencies.

We find qualitative agreement with Monte Carlo simulations for the density-density correlation function only when the spectrum does not present a complicated structure, i.e., in the strong coupling limit. However, the method presented here provides a way to obtain better numerical results using much less computing time. For example, all the results presented in Figs. 1 and 2 are obtained after $\simeq 5$ of CPU time. Most of this computer time is used to construct the ground state (which also contains valuable information not discussed here), only a little fraction is used to calculate a set of coefficients $\{a_n, b_n\}$. Typically 25 coefficients are enough to get accurate spectral functions.

We also have studied the current-current and the single-particle dynamical correlation functions. As we show in Sec. III, from this function we can calculate static properties of the systems. As an illustrative example we evaluate the binding energy of the exciton and show that the obtained results are a smooth interpolation between the weak and strong coupling limits.

We conclude that the technique presented here supplemented with the modified Lanczos algorithm for generating the ground state is an efficient way to study the properties of many-body systems at zero temperature.

ACKNOWLEDGMENTS

One of us (E.R.G.) would like to thank S. Bacci and B. Alascio for a critical reading of the manuscript. E.R.G. is supported by Consejo Nacional de Investigaciones Cientificas y Técnicas, Argentina.

[1]For a review see Proceedings of the Conference on Frontiers of Quantum Monte Carlo, Los Alamos, 1985 [J. Stat. Phys. **43**, 729 (1986)].

[2]D. J. Scalapino, J. Stat. Phys. **43**, 757 (1986); M. Suzuki *ibid.* **43**, 883 (1986).

[3]J. E. Hirsch and J. R. Schrieffer, Phys. Rev. B **28**, 5353 (1983).

[4]E. C. Behrmann, G. A. Jongeward, and P. G. Wolynes, J. Chem. Phys. **79**, 6277 (1983); D. Thirumvalai and B. Berme, *ibid.* **79**, 5029 (1983).

[5]H. B. Schülter and D. J. Scalapino, Phys. Rev. Lett. **55**, 1204 (1985); Phys. Rev. B **34**, 4744 (1986).

[6]E. R. Gagliano and C. A. Balseiro, Phys. Rev. Lett. **59**, 2999 (1987).

[7]M. H. Lee, Phys. Rev. B **26**, 2547 (1982); Phys. Rev. Lett. **49**, 1072 (1982); J. Math. Phys. **24**, 2512 (1983). Also see P. Grigolini, G. Grosso, G. Pastori Parravicini, and M. Sparpaglione, Phys. Rev. B **27**, 7342 (1983); M. Giordano, P. Grigolini, D. Leprini, and P. Martin, Phys. Rev. A **28**, 2474 (1983), and in *Memory Function Approaches to Stochastic Problems in Condensed Matter,* edited by M. V. Evans, P. Grigolini, and G. Pastori Parravicini (Wiley, New York, 1985), p. 133.

[8]R. Haydock, V. Heine, and M. J. Kelly, J. Phys. C **5**, 2845 (1972); **8**, 2591 (1975). See also the contributing papers of the same authors in *Solid State Physics,* edited by H. Ehrenreich, F. Seitz, and D. Turnbull (Academic, New York, 1980), Vol. 35.

[9]R. G. Gordon, J. Math. Phys. **9**, 655 (1968). See also G. Grosso and G. Pastori Parravicini in Ref. 7, p. 133.

[10]J. Florencio and M. H. Lee, Phys. Rev. B **35**, 1835 (1987).

[11]H. Mori, Prog. Theor. Phys. **33**, 423 (1965); **34**, 399 (1965).

[12]T. Jordan and E. Wigner, Z. Phys. **47**, 631 (1928).

[13]R. Bruinsma, P. Bak, and J. B. Torrance, Phys. Rev. B **27**, 456 (1983).

[14]E. R. Gagliano, A. G. Rojo, C. A. Balseiro, and B. Alascio, Solid State Commun. **64**, 901 (1987).

[15]J. des Cloizeaux and M. Gaudin, J. Math. Phys. **7**, 1384 (1966).

[16]For example see, W. P. Su, J. R. Schrieffer, and A. J. Heeger, Phys. Rev. B **22**, 2099 (1980).

[17]E. Dagotto and A. Moreo, Phys. Rev. D **31**, 865 (1985); E. R. Gagliano and S. Bacci, *ibid.* **36**, 546 (1987); E. R. Gagliano, E. Dagotto, A. Moreo, and F. Alcaraz, Phys. Rev. B **34**, 1677 (1987).

[18]W. Marshall and S. W. Lovesey, *Theory of Thermal Neutron Scattering* (Clarendon, Oxford, 1971).

[19]N. Ishimura and H. Shiba, Prog. Theor. Phys. **63**, 743 (1980).

[20]J. Villian, Physica B + C **79B**, 1 (1975); S. E. Nagler, W. J. L. Buyers, R. L. Armstrong, and B. Briat, Phys. Rev. Lett. **49**, 590 (1982).

[21]X-ray induced photoelectron spectroscopy (XPS) and bremsstrahlung-isochromat spectroscopy (BIS) are experimental techniques used to investigate the electronic structure. As an illustrative example see, N. Nücker, J. Fink, B. Renber, D. Ewert, C. Politis, P. J. W. Weijs, and J. C. Fuggle, Z. Phys. B **67**, 9 (1987).

[22]The number of holes ρ is evaluated numerically from Eq. (2.36) of Ref. 13.